Organometallics **2002,** *21,* 5531−5539

Nickel-Triflate Complexes as Precursors to Reactive Cations: Preparation and Reactivities of (1-R-indenyl)Ni(PPh$_3$)(OSO$_2$CF$_3$)

Ruiping Wang, Laurent F. Groux, and Davit Zargarian*

Département de Chimie, Université de Montréal, Montréal, Qucbec, Canada H3C 3J7

Received July 12, 2002

The complexes (1-R-indenyl)Ni(PPh$_3$)(OTf) (OTf = OSO$_2$CF$_3$; R = Et (**1**), *i*-Pr (**2**), and Bz (**3**)) have been prepared by reacting the corresponding Ni-thienyl or Ni-Cl precursors with HOTf (triflic acid) or AgOTf, respectively. The triflate ligand in these complexes undergoes facile displacement by various substrates or ligands to facilitate (a) catalytic dimerization of ethylene, isomerization of 1-hexene, and polymerization of phenylacetylene, or (b) formation of the cationic complexes [(1-R-indenyl)(PPh$_3$)Ni(L)]$^+$ (R = *i*-Pr (**a**) and CH$_2$Ph (**b**); L = CH$_3$CN (**4**), PhCN (**5**), CO (**6**), Py (**7**), CNC(CH$_3$)$_3$ (**8**), PPh$_3$ (**9**), and PMe$_3$ (**10**)). Compounds **1**−**10** have been characterized spectroscopically and, in the case of complexes **2**, **4a**, and **8a**, by single-crystal X-ray crystallography.

Introduction

The importance of transition metal-based cationic species in catalysis has been amply demonstrated in numerous studies on olefin polymerization,[1] CO/olefin copolymerization,[2] and organic synthesis.[3] Our own studies have implied that the cationic species [Ind(PPh$_3$)Ni]$^+$, which can be generated in-situ from Ind(PPh$_3$)NiX (Ind = indenyl and its substituted derivatives; X = halide or alkyl), might be the active catalyst for the oligomerization or polymerization of certain olefins.[4] However, the mechanistic details of these reactions have proven difficult to study, because the initiators needed for the in-situ generation of the active species often undergo unwanted reactions with both the substrates and the precatalysts. For example, Ag$^+$-based initiators themselves can promote cationic catalysis with some substrates such as styrene[5] and can oxidize some transition metal precursors.[6] To avoid such potential complications, we have set out to develop systems that can act as single-component precursors for the “initiatorless” generation of the cationic species [IndNi(PPh$_3$)]$^+$. Direct access to the latter species would be expected to simplify mechanistic studies of their reactions and should allow us to determine whether they are, indeed, the truly active species in the catalytic reactions.

In the search for direct access to our target cations, we have explored a strategy based on systems in which one coordination site around the Ni center is temporarily occupied by a hemilabile ligand; displacement of this ligand by various substrates would release the cationic species and initiate catalysis. The viability of this strategy has been demonstrated by preliminary studies which have shown that compounds such as [{η^3,η^1(N)-Ind-CH$_2$CH$_2$NMe$_2$}Ni(PPh$_3$)]$^+$ catalyze the cationic polymerization of styrene thanks to the hemilabile coordination of the tethered amine moiety.[7] One drawback of this system is that the intramolecular coordination of the amine moiety is fairly competitive with the intermolecular coordination of the substrate molecules; as a result, catalysis with this system requires forcing conditions and is limited to reactive substrates (e.g., polymerization of styrene proceeds at high temperatures only).

While our investigations aimed at improving the catalytic activities of the above-described systems continue, we have also examined an alternative approach based on using complexes bearing nonchelating, weakly nucleophilic ligands such as triflate as precursors to highly reactive cationic intermediates.[8] The present report describes the preparation and characterization of the triflate derivatives (1-R-Ind)(PPh$_3$)Ni(OTf) (R = Et (**1**), *i*-Pr (**2**), and Bz (**3**)) and discusses their reactivities with ethylene, 1-hexene, phenylacetylene, and phenylsilane. The facile substitution of the OTf moiety in these complexes has given access to the new cationic

---

(1) (a) Johnson, L. K.; Killian, C. M.; Brookhart, M. *J. Am. Chem. Soc.* **1995**, *117*, 6414. (b) Mathew, J. P.; Reinmuth, A.; Melia, J.; Swords, N.; Risse, W. *Macromolecules* **1996**, *29*, 2755. (c) Gottfried, A. C.; Brookhart, M. *Macromolecules* **2001**, *34*, 1140. (d) Britovesk, G. J. P.; Gibson, V. C.; Wass, D. M. *Angew. Chem., Int. Ed.* **1999**, *38*, 428. (e) Ittel, S. D.; Johnson, L. K.; Brookhart, M. *Chem. Rev.* **2000**, *100*, 1169. (f) Mecking, S. *Coord. Chem. Rev.* **2000**, *203*, 325. (g) Svejda, S. A.; Johnson, L. K.; Brookhart, M. *J. Am. Cehm. Soc.* **1999**, *121*, 10634. (h) Hlatky, G. G.; Turner, H. W.; Eckman, R. R. *J. Am. Chem. Soc.* **1989**, *111*, 2728. (i) Jordan, R. F. *J. Chem. Educ.* **1988**, *65*, 285. (j) Sen, A.; Lai, T.-W. *Organometallics* **1982**, *1*, 415. (k) Eisch, J. J.; Piotrowski, A. M.; Brownstein, S. K.; Gabe, E. J.; Lee, F. L. *J. Am. Chem. Soc.* **1985**, *107*, 7219. (l) Jordan, R. F.; Bajgur, C. S. Willett, R.; Scott, B. *J. Am. Chem. Soc.* **1986**, *108*, 7410.

(2) (a) Bianchini, C.; Meli, A. *Coord. Chem. Rev.* **2002**, *225*, 35. (b) Sen, A. *Acc. Chem. Res.* **1993**, *26*, 303. (c) Drent, E.; Budzellar, P. *Chem. Rev.* **1996**, *96*, 663.

(3) (a) Bosnich, B. *Aldrichim. Acta* **1998**, *31*, 76. (b) Suzuki, K. *Pure Appl. Chem.* **1994**, *66*, 1557.

(4) (a) Vollmerhaus, R.; Bélanger-Gariépy, F.; Zargarian, D. *Organometallics* **1997**, *16*, 4762. (b) Fontaine, F.-G.; Zargarian, D. Unpublished results. (c) The analogous allyl nickel complexes (allyl)Ni(PR$_3$)Cl also dimerize ethylene and propylene in the presence of initiators such as AlEtCl$_2$: Wilke, G. *Angew. Chem., Int. Ed. Engl.* **1988**, *27*, 185.

(5) Hermans, J. P.; Smets, G. *J. Polym. Sci., Part A* **1965**, *3*, 3175.

(6) Jordan, R. F.; LaPointe, R. E.; Bajgur, C. S.; Echols, S. F.; Willett, R. *J. Am. Chem. Soc.* **1987**, *109*, 4111.

(7) Groux, L. G.; Zargarian, D. *Organometallics* **2001**, *20*, 3811.

10.1021/om020558a CCC: $22.00

Scheme 1

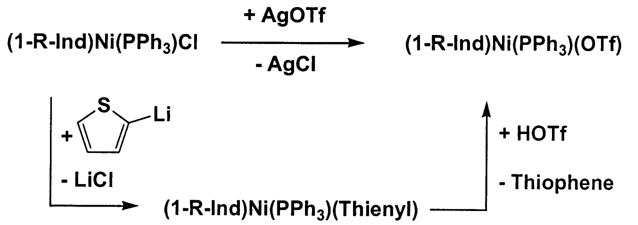

Scheme 2

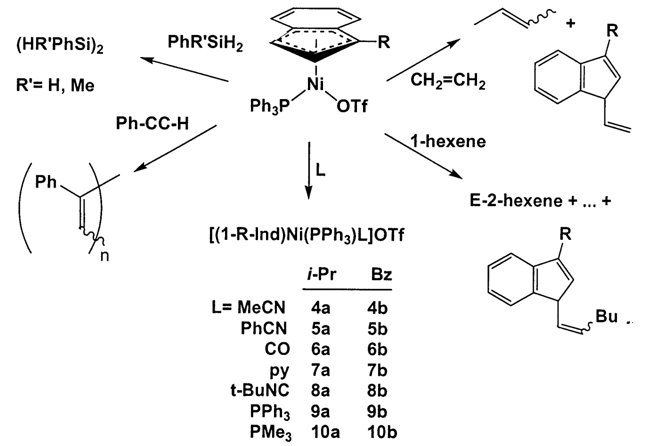

	i-Pr	Bz
L= MeCN	4a	4b
PhCN	5a	5b
CO	6a	6b
py	7a	7b
t-BuNC	8a	8b
PPh$_3$	9a	9b
PMe$_3$	10a	10b

complexes [(1-R-indenyl)(PPh$_3$)Ni(L)]$^+$ (R = *i*-Pr (**a**) and CH$_2$Ph (**b**); L = CH$_3$CN (**4**), PhCN (**5**), CO (**6**), Py (**7**), CNC(CH$_3$)$_3$ (**8**), PPh$_3$ (**9**), and PMe$_3$ (**10**)), which are also described herein.

Results and Discussion

Synthesis and Characterization of (1-R-Ind)Ni(PPh$_3$)(OTf). Complexes **1**−**3** were prepared by two related approaches. First, the corresponding thienyl complexes were treated with 1 equiv of triflic acid to give thiophene and the triflate derivatives as red powders in ca. 45% yield. A somewhat higher yielding (50−60%) and more direct path to the triflate compounds involves the reaction of the chloro precursors with an excess of AgOTf (Scheme 1). It is interesting to note that the 1-Et-, 1-*i*-Pr-, and 1-Bz-Ind derivatives are relatively easy to isolate, whereas the 1-Me-Ind analogue decomposes during isolation to [(1-Me-Ind)Ni(PPh$_3$)$_2$]$^+$. This dependence of stability on the increasing steric bulk of the Ind substituent might imply that the decomposition proceeds via an associative (presumably solvent-assisted) displacement reaction instead of a unimolecular dissociation of OTf.

The structures of complexes **1**−**3** have been deduced from their NMR and IR spectra and confirmed by the results of single-crystal X-ray diffraction studies carried out on complexes **2** and **3**. The main spectroscopic features of the OTf complexes are as follows. The observation of an asymmetric sulfonyl stretching mode at 1324 cm^{-1} in the IR spectra and a singlet resonance at ca. −80 ppm in the ^{19}F NMR spectra of **1**−**3** support the presence in these compounds of an η^1-coordinated triflate group.[9] The ^{1}H NMR spectra exhibit the anticipated signals for the diastereotopic IndCH_2 and IndCH(CH_3)$_2$ protons. Comparison to the ^{1}H NMR spectra of the precursors revealed that the signals for H3 (labeling shown on ORTEP figures) resonate more upfield in **1**−**3** than in the Ni-thienyl (ca. 4.0 ppm) and Ni-Cl (ca. 3.3 ppm) analogues. The same trend is also observed for the ^{31}P{^{1}H} NMR signals: 29 ppm for the OTf complexes versus 37 and 31 ppm for the thienyl and Cl analogues, respectively. These findings are consistent with an empirical trend we have noted[10] for the complexes IndNi(PPh$_3$)(X), according to which the ^{1}H and ^{31}P NMR signals due to H3 and PPh$_3$ both move upfield as the nucleophilicity of the ligand X decreases (Me > Et > CC-Ph, 2-thienyl > PhS, phthalimidate, I > Br > Cl > OTf). Comparing the solution NMR data for the OTf complexes **1**−**3** to those obtained previously for this family of indenyl nickel complexes allows us to predict relatively long Ni−P distances and nonsymmetrical (η^1, η^2) Ind-Ni bonding in their solid state structures. These predictions are borne out by the results of the crystallographic studies carried out on **2** and **3**, which will be discussed later along with the solid state structures of the cationic adducts derived from these complexes (vide infra).

Trifalte Substitution Reactions. We were interested in the possibility of converting the OTf complexes into cationic complexes or reactive intermediates via the exchange of the OTf moiety by ligands of varying nucleophilicities (PR$_3$, CO, :CNR, :NCR, olefins, alkynes, silanes, etc.). Experiments showed that displacement of OTf by a variety of ligands takes place at room temperature to give the corresponding cationic complexes [(1-R-Ind)Ni(PPh$_3$)(L)][OTf] or initiate catalysis (Scheme 2). A description of the new cationic adducts is presented below, followed by a discussion of the reactivities of the Ni-OTf precursors with some substrates. Although the kinetics of these reactions have not been studied yet, we suspect that displacement of OTf in these compounds proceeds via an associative mechanism similar to that of phosphine substitution in the Ni-Cl analogues.[11]

[(1-R-Ind)Ni(PPh$_3$)L]$^+$. A number of cationic complexes have been obtained from the displacement of the OTf moiety in complexes **1**−**3** by various ligands L (L = CH$_3$CN (**4**), PhCN (**5**), CO (**6**), Py (**7**), CNC(CH$_3$)$_3$ (**8**), PPh$_3$ (**9**), and PMe$_3$ (**10**)). Monitoring by NMR showed that most of the OTf substitution reactions are very rapid and give the expected products quantitatively; however, reactions involving the ligands :CNBu^t and CO gave additional products, which will be discussed separately (vide infra). Compounds **4a**, **6a**, **7a**, **8a**, and **9a** have been isolated as yellow solids in ca. 50−75% yields. Complete characterization by NMR and IR spectroscopy and, in the case of **4a** and **8a**, by X-ray crystallorgraphy

---

[8] The facile dissociation of the triflate ligand under mild conditions is known to generate reactive cations. For some examples of the use of triflate compounds as precursors to strong Lewis acids in organic synthesis see: (a) Kobayashi, S.; Hachiya, I.; Takahori, T. *Synthesis* **1993**, 371, and references therein. (b) Hollis, T. K.; Bosnich, B. *J. Am. Chem. Soc.* **1995**, *117*, 4570, and references therein. (c) Tanabe, Y.; Mukaiyama, T. *Chem. Lett.* **1984**, 1867. (d) Tanabe, Y.; Mukaiyama, T. *Chem. Lett.* **1984**, 673. For some examples of the use of triflate complexes as precursors to cationic intermediates reactive toward C−H bonds see: (e) Burger, P.; Bergman, R. G. *J. Am. Chem. Soc.* **1993**, *115*, 10462. (f) Alaimo, P. J.; Bergman, R. G. *Organometallics* **1999**, *18*, 2707. (g) Alaimo, P. J.; Arndtsen, B. A.; Bergman, R. G. *Organometallics* **2000**, *19*, 2130.

[9] (a) Lawrance, G. A. *Chem. Rev.* **1986**, *86*, 17. (b) Braun, T.; Parsons, S.; Perutz, R. N.; Voith, M. *Organometallics* **1999**, *18*, 1710.

[10] Zargarian, D. *Coord. Chem. Rev.* **2002**, in press.

[11] Fontaine, F.-G.; Dubois, M.-A.; Zargarian, D. *Organometallics* **2001**, *20*, 5156.

has confirmed the structural features attributed to these complexes and, by extension, to the analogues which have been studied by spectroscopy only. Some of the observed spectroscopic features reveal important bonding patterns and will be discussed below.

The $^{31}P\{^1H\}$ NMR spectra of the cations **4**−**8** show the expected singlet resonance for the PPh_3 ligand in a narrow chemical shift range (32−38 ppm), while the spectra of complexes **9** and **10** show additional signals reflecting the presence of two inequivalent phosphine ligands. For example, an AB pattern ($^2J_{P-P} = 25.5$ Hz) was observed for complexes **9**; this is in agreement with the inequivalence of the two PPh_3 groups caused by the absence in these molecules of a plane of symmetry. For complexes **10**, we observed an AA′BB′ pattern ($^2J_{P-P} = 42$ Hz) attributed to the two rotamers of each molecule, one rotamer with the Ind substituent above PMe_3, the other above PPh_3. These spectral patterns are consistent with those reported previously for the 1-Me-Ind analogues.[4a] The $^{13}C\{^1H\}$ NMR spectra displayed the expected signals for Ind and PPh_3 carbons in addition to those for ligands L. For instance, the CO adduct **6a** gave rise to a doublet at ca. 190 ppm ($^2J_{P-C} = 16.8$ Hz).

The ^1H NMR spectra of the new complexes also contained the expected signals for L, in addition to the PPh_3 and Ind signals characteristic of this family of complexes. For instance, in the case of the CH_3CN adduct **4a** a singlet at 1.99 ppm was assigned to CH_3CN; the absence of this signal in the ^1H NMR of the CD_3CN adduct (**4a′**) confirmed this assignment. As discussed earlier for the Ni-OTf complexes, the chemical shift of the signal for H3 is particularly informative on the Ind hapticity in these complexes. For instance, previous studies have shown[10,12] that for the complexes $IndNi(PR_3)X$ strong donor ligands X (e.g., alkyl groups) bring about increasingly symmetrical coordination of the Ind ligand; this, in turn, results in more downfield signals for H3, consistent with greater sp^2 character on C3. A comparison of the H3 chemical shifts for the cationic adducts reveals a similar pattern; that is, strong ligands give rise to more downfield signals: CO (5.53 ppm) > PPh_3 (5.13 ppm) > $CNC(CH_3)_3$ (4.80 ppm) > PhCN (4.30 ppm) ≈ Py (4.21 ppm) ≈ CH_3CN (4.18 ppm). This order roughly parallels the donating strengths of these ligands to late metals.[13]

Finally, the frequencies of the ν(CN) and ν(CO) bands in the IR spectra of complexes **4**, **6**, and **8** can be used to estimate the extent of π-back-bonding between the ligand L and the Ni center in these cations. Thus, the energy of the ν(CN) absorption band in **4a** (2251 cm^{-1}) is little changed from its value in free MeCN (2275 cm^{-1}), implying only a small degree of π-back-bonding between this weakly π-acidic ligand and the cationic Ni center. In contrast, the energy of the ν(CO) absorption band in **6a** (2089 cm^{-1}) is significantly lower than that of free CO (2149 cm^{-1})[14] and intermediate between the corresponding values reported for the anionic complex $[Ni(CO)(SR)_3]^-$ (2043 cm^{-1}; R = 2-thienyl)[15] and the cationic complex $[(PPh_3)_2PtCl(CO)]^+$ (2100 cm^{-1}).[16] We conclude that there is a fairly strong π-back-bonding between CO and Ni in complex **6a**. Interestingly, the ν(CN) absorption band in **8a** (2196 cm^{-1}) is at a higher energy than the free ligand (2136 cm^{-1}). This observation is consistent with the notion that removal of electron density from the isocyanide ligand's "lone pair" (or $5\sigma'$ orbital), which has some degree of antibonding character with respect to the C−N bond, results in an increase in the C−N bond order.[17] Thus, the high energy of the ν(CN) absorption band in **8a** is likely caused by the strong σ-donation from :$CNBu^t$ to the cationic Ni center in **8a**. It is noteworthy that a large ν(CN) value (2175 cm^{-1}) is also reported for the analogous (but neutral) complex $(\eta^5\text{-}C_2B_9H_{10}CH_2NMe_2)Ni(CNBu^t)$,[18] thus confirming that isocyanide ligands are stronger σ-donors and weaker π-acceptors compared to CO.

Scheme 3

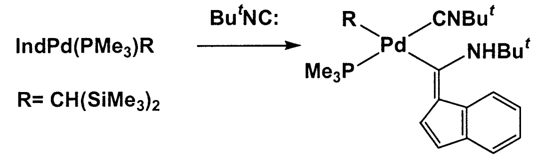

As mentioned earlier, reactions of the OTf complexes with CO and :$CNBu^t$ gave species other than the simple OTf substitution products. In the case of the CO reactions, for instance, the IR spectra showed a second, less intense absorption band at ca. 1995 cm^{-1} along with the main absorption band for the anticipated CO complex. In the case of the :$CNBu^t$ reactions, the $^{31}P\{^1H\}$ NMR spectra of the reaction mixtures showed that using substoicheometric amounts of ligand gives only the products of the simple substitution reaction (signals at 38.11 and 38.25 ppm for **8a** and **8b**, respectively); on the other hand, using one or more equivalents of :$CNBu^t$ gives increasing amounts of a second species that displayed new signals at 49.50 and 49.49 ppm, respectively, for the reactions of **2** and **3**. We suspect that the unidentified products of these reactions are the complexes *trans*-$[(\eta^1\text{-}1\text{-}R\text{-}Ind)(PPh_3)NiL_2]^+$ (L = CO, $CNBu^t$), which would arise from the coordination of a second equivalent of the isocynaide or CO ligands and the concomitant slippage of the Ind ligand to an η^1 mode. This proposal is based on a similar reactivity reported for the reaction of the complex $(\eta\text{-}Ind)Pd(PMe_3)(CH_2SiMe_3)$ with :$CNBu^t$, which gives the indenylfulvene product shown in Scheme 3. The course of the latter reaction involves slippage of the Ind ligand ($\eta^3 \rightarrow \eta^1$) caused by the coordination of two :$CNBu^t$ molecules, followed by insertion of one :$CNBu^t$ into the Pd−(η^1-Ind) bond and H-shift.[19] We believe that in the case of our complexes the insertion step does not take

---

(12) (a) Huber, T. A.; B.-Gariépy, F.; Zargarian, D. *Organometallics* **1995**, *14*, 4997. (b) Bayrakdarian, M.; Davis, M. J.; Reber, C.; Zargarian, D. *Can. J. Chem.* **1996**, *74*, 2115. (c) Huber, T. A.; Bayrakdarian, M.; Dion, S.; Dubuc, I.; B.-Gariépy, F.; Zargarian, D. *Organometallics* **1997**, *16*, 5811. (d) Dubuc, I.; Dubois, M.-A.; Bélanger-Gariépy, F.; Zargarian, D. *Organometallics* **1999**, *18*, 30. (e) Wang, R.; Bélanger-Gariépy, F.; Zargarian, D. *Organometallics* **1999**, *18*, 5548.

(13) Collman, J. P.; Hegedus, L. S.; Norton, J. R.; Fink, R. G. *Principles and Applications of Organotransition Metal Chemistry*; University Science Book: Mill Valley, CA, 1987; p 243.

(14) Crabtree, R. H. *The Organometallic Chemistry of the Transition Metals*, 2nd ed.; John Wiley & Sons: New York, 1994; p 15.

(15) Liaw, W.; Chen, C.; Lee, C.; Lee, G.; Peng, S. *J. Chem. Soc., Dalton Trans.* **2001**, 138.

(16) Collman, J. P.; Hegedus, L. S.; norton, J. R.; Finke, R. G. *Principles and Applications of Organotransition Metal Chemistry*; University Science Books: Mill Valley, CA, 1987; p 114.

(17) Treichel, P. M. *Adv. Organomet. Chem.* **1973**, *11*, 21.

(18) Park, J.; Kim, D.; Kim, S.; Ko, J.; Kim, S.; Cho, S.; Lee, C.; Kang, S. *Organometallics* **2001**, *20*, 4483.

Table 1. Crystal Data Collection and Refinement Parameters for Complexes 2, 4a, and 8a

	2	**4a**·$CHCl_3$	**8a**
formula	$C_{31}H_{28}F_3NiO_3PS$	$C_{33}H_{31}F_3NO_3PS{\bullet}CHCl_3$	C36H37F3NiO3PS
mol wt	627.274	787.696	710.406
cryst color	dark red	dark yellow	dark red
cryst habit	block	block	block
cryst dimens, mm	0.74 × 0.48 × 0.24	0.76 × 0.49 × 0.37	0.46 × 0.40 × 0.27
cell setting	monoclinic	triclinic	orthorhombic
space group	$P2_1/n$	$P\bar{1}$	*Pbca*
a, Å	9.1834(1)	10.6791(1)	13.571(3)
b, Å	20.6114(1)	12.8546(1)	18.681(4)
c, Å	15.5120(1)	14.1394(1)	28.083(6)
α, deg		76.855(1)	
β, deg	98.002(1)	75.202(1)	
γ, deg		79.150(1)	
V, Å^3	2907.57(2)	1809.90(3)	7120(2)
Z	4	2	8
D(calcd), g cm^{-3}	1.4330	1.4454	1.3255
λ(Cu Kα), cm^{-1}	1.54178	1.54178	1.54178
temp, K	298(2)	223(2)	293(2)
diffractometer	Bruker AXS SMART	Bruker AXS SMART	Nonius CAD-4
$2\theta_{max}$, deg	146.16	145.76	139.98
data collecn method	$\omega/2\theta$ scan	$\omega/2\theta$ scan	$\omega/2\theta$ scan
no. of reflns used ($I > 2\sigma(I)$)	5556	6194	2847
R, R_w	0.0460, 0.1277	0.0604, 0.1681	0.0353, 0.0484

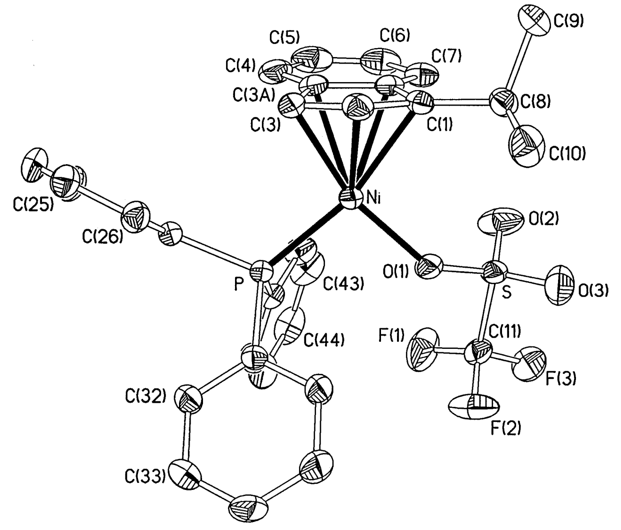

Figure 1. ORTEP view of complex **2** with atom labeling; ellipsoids show 40% probability levels, and hydrogen atoms have been omitted for clarity.

Table 2. Selected Bond Distances (Å) for (1-*i*-Pr-Ind)Ni(PPh$_3$)(OTf) (2), [(1-*i*-Pr-Ind)Ni(PPh$_3$)(NCCH$_3$)]OTf (4a), and [(1-*i*-Pr-Ind)Ni(PPh$_3$)(CNC(CH$_3$)$_3$)]OTf (8a)

	7	**9a**	**13a**
Ni−P	2.1973(6)	2.1918 (6)	2.1838(9)
Ni−(O1, N1, C11)	1.9404(16)	1.869(2)	1.816(3)
Ni−C1	2.131(2)	2.128(2)	2.082(3)
Ni−C2	2.064(2)	2.064(2)	2.066(3)
Ni−C3	2.024(2)	2.013(2)	2.038(3)
Ni−C3a	2.311(2)	2.283(2)	2.248(3)
Ni−C7a	2.335(2)	2.326(2)	2.248(3)
C1−C2	1.410(3)	1.410(3)	1.409(3)
C2−C3	1.412(4)	1.405(4)	1.405(3)
S−O1	1.4543(17)		
S−O2	1.400 (2)		
S−O3	1.422(2)		
S−C11	1.822(3)		
C11−F1	1.287(3)		
N1−C12		1.132(4)	
C12−C13		1.464(4)	
C11−N			1.144(3)
C12−N			1.464(3)
C12−C13			1.496(7)
ΔM−C[a]	0.25	0.23	0.19

[a] Δ(M−C) = $^1/_2$[(Ni−C3a + Ni−C7a) − (Ni−C1 + Ni−C3)].

place since the NMR spectra of the side products contain the signal due to the Ind H3 proton.

Solid State Structures of 2, 4a, and 8a. The solid state structures of complexes **2**, **3**, **4a**, and **8a** have been determined (R (%) = 4.6, 6.34, 6.04, and 3.53, respectively). The geometry around the Ni center in these complexes is intermediate between a two-legged piano stool (with $\eta^3 \leftrightarrow \eta^5$-Ind) and distorted square planar (with $\eta^1,\eta^2 \leftrightarrow \eta^3$-Ind). Some of the important structural features of these complexes are described below; the structure of complex **3** has been described elsewhere[20] and will not be discussed in detail here.

The ORTEP diagram for **2** is shown in Figure 1. The crystal data and refinement parameters are summarized in Table 1, while the bond distances and angles are given in Table 2 and Table 3, respectively. No rotational disorder was detected for the triflate ligand in **2**, in contrast to what has been observed for a majority of OTf compounds, including complex **3**. The Ni−O distance of 1.9404(16) Å in **2** is comparable to the corresponding distances in **3** (1.972(9) Å) and *trans*-[Ni(OTf)(2-C_5F_4N)(PEt$_3$)$_2$] (1.957(2) Å), but longer than the Ni−O distance in [Ni(OPh)(2-C_5F_4N)(PEt$_3$)$_2$] (1.894(4) Å);[21] this is consistent with the low nucleophilicity of OTf compared to OPh. The long Ni−C3a/7a distances (av 2.32 Å) imply a significant $\eta^5 \rightarrow \eta^3$ distortion (ΔM−C = 0.25 Å),[22] whereas the unequal Ni−C1 and Ni−C3

---

(19) Alias, F. M.; Belderrain, T. R.; Paneque, M.; Poveda, M. L.; Carmona, E. *Organometallics* **1998**, *17*, 5620.

(20) Wang, R.; Groux, L. F.; Zargarian, D. *J. Organomet. Chem.* **2002**, in press.

(21) Braun, T.; Parsons, S.; Perutz, R. N.; Voith, M. *Organometallics* **1999**, *18*, 1710.

Table 3. Selected Bond Angles (deg) for (1-*i*-Pr-Ind)Ni(PPh_3)(OTf) (2), [(1-*i*-Pr-Ind)Ni(PPh_3)($NCCH_3$)]OTf (4a), and [(1-*i*-Pr-Ind)Ni(PPh_3)($CNC(CH_3)_3$)]OTf (8a)

	2	4a	8a
O1(N1, C11)−Ni−P	96.41(6)	99.29(6)	96.41(8)
O1(N1)−Ni−C3	163.74(9)	161.31(10)	161.54(12)
C3−Ni−P	99.63(7)	99.16(8)	102.2(9)
O2−S−O1	115.50(14)		
O2−S−C11	106.13(15)		
O2−S−O3	115.28(19)		
O3−S−O1	113.07(14)		
N1−C12−C13		178.7(3)	
Ni−N1−C12		172.6(2)	
Ni−C11−N			176.3(3)
C11−N−C12			178.4(3)
N−C12−C13			110.4(6)
FA[a]	9.19(0.12)	8.13(0.17)	7.69(0.20)
HA[a]	10.50(0.12)	10.63(0.18)	10.06(0.22)

[a] HA (hinge angle) = angle between the planes defined by C1, C2, C3 and C1, C3, C3a, C7a; FA (fold angle) = angle between the planes defined by C1, C2, C3 and C3a, C4, C5, C6, C7, C7a.

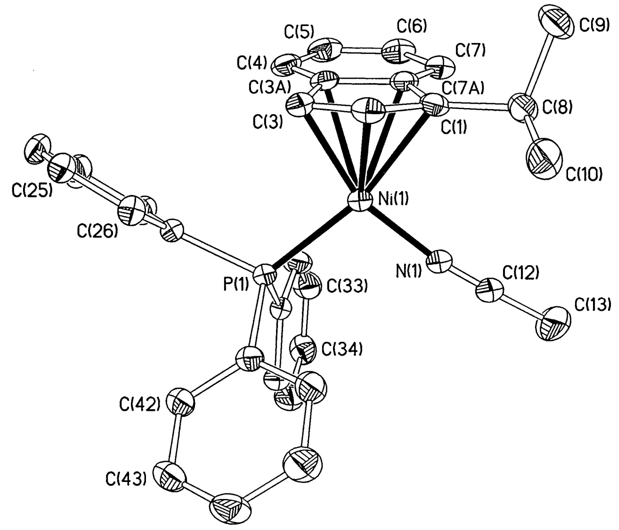

Figure 2. ORTEP view of complex **4a**·$CHCl_3$ with atom labeling; ellipsoids show 30% probability levels. The anion, solvent, and hydrogen atoms have been omitted for clarity.

distances reflect the much greater trans influence of PPh_3 compared to the OTf ligand.

The ORTEP diagrams for complexes **4a** and **8a** are shown in Figures 2 and 3, respectively; the OTf anions, which are disordered over two (in **4a**) and three (**8a**) sets of positions, have been omitted for clarity. Rotational disorders were also observed for the cocrystallized molecule of $CHCl_3$ in **4a** and the methyl groups of the *t*-Bu fragment in **8a**. The acetonitrile and isocyanide ligands are essentially linear: for **4a**, the Ni−N1−C12 and N1−C12−C13 angles are ca. 173° and 179°, respectively, while N1−C12 is ca. 1.13 Å; for **8a**, the Ni−C11−N and C11−N−C12 angles are ca. 176° and 178°, respectively, while C11−N is ca. 1.14 Å. The Ni−N and N−C bond lengths are fairly similar in the acetonitrile adduct **4a** (1.869(2) and 1.132(4) Å, respectively) and the neutral complex (η^5-Cp)Ni{Sn(CH($SiMe_3$)$_2$)(OH)}(CH_3CN)[23] (1.829(3) and 1.138(5) Å, respectively). On the other hand, the Ni−C11 bond distance of 1.816(3) Å in the isocyanide adduct **8a** is shorter than the corresponding Ni−C(sp) bond distance of 1.861(4) Å in the neutral alkynyl analogue (1-Me-Ind)(PPh_3)Ni(CC-Ph),[12e] consistent with the strong interaction between Ni and the isocyanide ligand as deduced from the IR data (vide supra).

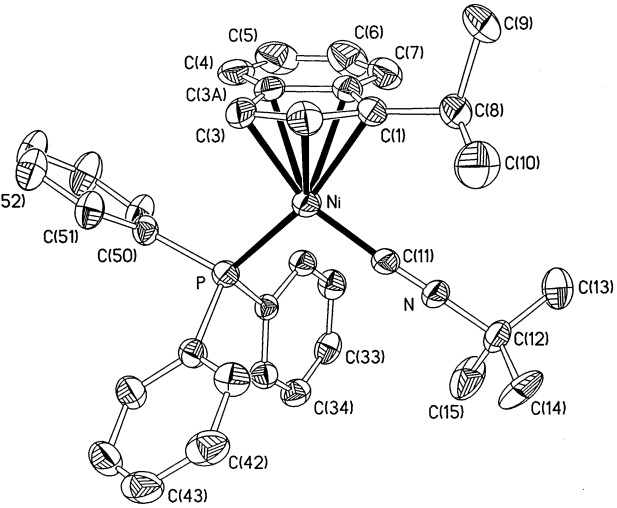

Figure 3. ORTEP view of complex **8a** with atom labeling; ellipsoids show 30% probability levels. The anion and hydrogen atoms have been omitted for clarity.

Previous structural studies carried out on the neutral and cationic compounds [Ind(PPh_3)Ni(X or L)]$^{n+}$ ($n = 0$ with X; 1 with L) have shown that the more strongly donating ligand X/L results in a shorter Ni−P distance and stronger, more symmetrical Ni−Ind interactions.[10,12] Consistent with this trend, complexes **2**, **4a**, and **8a** show Ni−P distances of 2.1973(6), 2.1918(6), and 2.1838(9) Å, respectively, and ΔM−C values of 0.25, 0.23, and 0.19 Å, respectively; these data reflect the relative nucleophilicities of the ligands involved (OTf < MeCN < (*t*-Bu)NC). On the other hand, the observed values of the Ni−C3a and Ni−C7a bond lengths can be explained in terms of the relative trans influences of PPh_3 and the other ligands. Thus, the greater trans influence of PPh_3 compared to OTf and MeCN gives rise to somewhat longer Ni−C7a versus Ni−C3a bonds in **2** (2.335(2) vs 2.311(2) Å) and **4a** (2.283(2) vs 2.326(2) Å), while the similar trans influences of PPh_3 and :$CNBu^t$ results in symmetrical distances in **8a** (2.248(3) Å). Finally, it is important to note that the Ind hapticity observed in the solid state structure of each complex is maintained in the solution, as discerned from the $^{13}C\{^1H\}$ NMR chemical shifts for C3a and C7a, with more upfield shifts indicating more η^5-like hapticity for the Ind ligand.[22a,b] Thus, comparison of δ_{av}(C3a/C7a) values shows that the Ind hapticity in these complexes increases on going from **2** (126.4 ppm) to **4a** (124.7 ppm) to **8a** (121.3 ppm).

Reactivities of the OTf Complexes with 1-Hexene and Ethylene. The reaction of the Ni-OTf complex **2** with 50 equiv of 1-hexene (1.3 M in $CDCl_3$) led to the formation of 2-hexene over 24 h at room temperature. The GC/MS analysis of the final mixture did not detect

---

[22] For a definition of ΔM−C see footnote of Table 2; for a comparison of ΔM−C values for M-Ind compounds see: (a) Westcott, S. A.; Kakkar, A. K.; Stringer, G.; Taylor, N. J.; Marder, T. B. *J. Organomet. Chem.* **1990**, *394*, 777. (b) Baker, R. T.; Tulip, T. H. *Organometallics* **1986**, *5*, 839.

[23] Schneider, J. J.; Hagen, J.; Bläser, D.; Boese, R.; Fabrizi de Biani, F.; Zanello, P. Krüger, C. *Eur. J. Inorg. Chem.* **1999**, 1987.

any dimers or oligomers, showing instead hexene as the main component, in addition to traces of 1,3-(hexenyl, *i*-Pr)-indene ($M^{\bullet+}$ = 240; $M^{\bullet+}$ − 15 (CH_3); $M^{\bullet+}$ − 29 (CH_2CH_3); $M^{\bullet+}$ − 43 (Pr or *i*-Pr); $M^{\bullet+}$ − 57 (Bu); etc.). The $^{13}C\{^1H\}$ NMR spectrum exhibited two sets of six peaks; comparison of these signals to literature values indicated that the major set corresponds to *E*-2-hexene,[24] whereas the minor set closely resembles, but is not the same as, the literature values for *Z*-2-hexene.[25] This minor product is likely an isomer of hexene, but its precise identity has not been confirmed yet.

GC/MS analyses of solutions of **2** (ca. 0.02 M) through which ethylene had been bubbled for ca. 5 min indicated the formation of butene(s). Similar experiments were carried out in $CDCl_3$ (0.03 M) with complexes **1** or **2** in order to analyze the reaction mixture in-situ by NMR. The ^1H and $^{13}C\{^1H\}$ NMR spectra of these reactions showed the presence of *E*- and *Z*-2-butene (ca. 4:1),[26] while the $^{31}P\{^1H\}$ NMR spectra showed the presence of mainly **2** plus a small amount of $[(1\text{-Pr}^i\text{-Ind})Ni(PPh_3)_2]^+$ (vide supra). GC/MS analyses of these NMR samples confirmed the presence of butene(s) as well as 1,3-(vinyl, *i*-Pr)-indene ($M^{\bullet+}$ = 184; $M^{\bullet+}$ − 15 (CH_3); $M^{\bullet+}$ − 30 (2 CH_3); $M^{\bullet+}$ − 43 (*i*-Pr); etc.) and 1,3-(vinyl, Et)-indene ($M^{\bullet+}$ = 170; $M^{\bullet+}$ − 15 (CH_3); $M^{\bullet+}$ − 29 (CH_3CH_2); etc.).

Taken together, the above results demonstrate that the Ni-OTf complexes are precatalysts for the dimerization of ethylene and isomerization of 1-hexene. These reactions are likely initiated via the displacement of OTf to form the cationic olefin adduct shown in Scheme 4. The coordination of a second molecule of olefin forces the Ind ligand into a monohapto mode, followed by the insertion of one of the coordinated olefins into the Ni−(1-R-Ind) bond to give $[L_nNi\{CHR'CH_2(R\text{-Ind})\}]^+$. The latter can then undergo β-H elimination to give the disubstituted indenes, which were detected by GC/MS analyses, and generate a cationic hydride that is probably the active catalyst for the dimerization of ethylene and the isomerization of 1-hexene (Scheme 4). No dimerization is observed with 1-hexene presumably because the β-H elimination from the initial product of insertion (i.e., $[L_nNi\text{-hexyl}]^+$) is faster than the coordination of a second molecule of hexene followed by insertion.

Reactivities of the OTf Complexes with PhCCH, $PhSiH_3$, and $PhSiMeH_2$. The activity of the OTf complexes in alkyne polymerization was studied by reacting complex **2** with 200 equiv of Ph-CC-H (in THF or neat) at 50 °C. The resulting, sparingly soluble yellow powder (ca. 5% yield) was shown to be poly(phenylacetylene) by GPC analysis (M_w = 8189, M_n = 4418, M_w/M_n = 1.85). The low solubility and molecular weight of this material, as well as its featureless ^1H NMR spectrum (broad signals at ca. 6.5−7.8 ppm), contrast with the properties of the *cis,transoidal*-poly(phenylacetylene) obtained previously[12e] from a combination of (1-Me-Ind)(PPh_3)Ni-X and MAO (X = Cl or CC-Ph; Ni:Al ratio 1:10); the latter polymers are soluble, have M_w of ca. (3−5) × 10^4, and show relatively sharp signals in the vinylic region of the ^1H NMR spectrum. These findings imply that the active species generated in the MAO-cocatalyzed reactions[12e] are not the same as the cationic species studied here.

Scheme 4

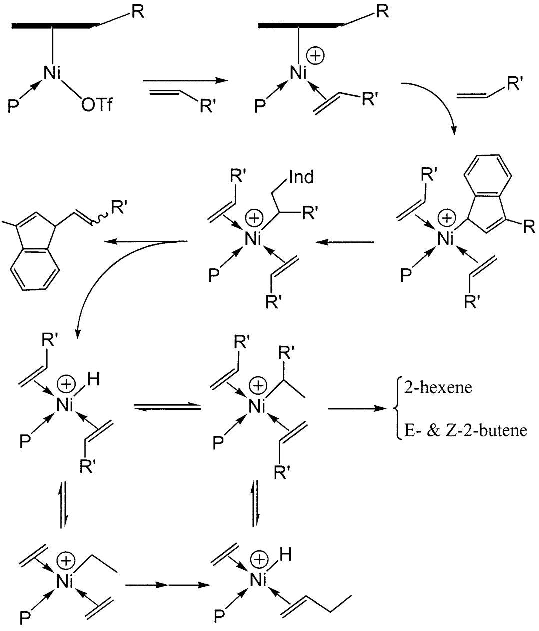

The reactivity of **2** with hydrosilanes was probed briefly by studying the reactions with $PhSiH_3$ and $PhMeSiH_2$. Addition of **2** to these silanes (both neat and in C_6D_6 solutions) resulted in the evolution of H_2; the ^1H NMR spectra of the final mixtures showed signals characteristic of the dimers of these silanes.[27] These results show that the cationic precursors tend to dimerize hydrosilanes, in contrast to the oligomerization activities observed with neutral Ni-Me precursors.[28] It is worth noting that the silane reactions do not seem to turn over, as they give very low conversions (ca. 2 equiv of silane consumed). Monitoring these reactions by ^1H NMR spectroscopy did not result in the detection of Ni-H resonances, but the $^{31}P\{^1H\}$ NMR spectra showed the emergence of a few singlets at ca. 35−40 ppm. We suspect that these resonances might be due to Ni-silyl intermediates, because derivatives bearing strong σ-donor ligands such as alkyl, alkenyl, and alkynyl ligands show ^{31}P signals in the region of 37−48 ppm.

Conclusion

The present study has shown that the OTf compounds (1-R-Ind)Ni(PPh_3)(OTf), which are prepared from the corresponding Ni-Cl or Ni-thienyl precursors, can serve as single-source precursors for generating highly electrophilic cations that dimerize ethylene, $PhSiH_3$, and

---

[24] The observed peaks: 13.6, 17.9, 22.7, 34.8, 124.7, and 131.4 ppm; the literature values for *E*-2-hexene: 13.7, 17.7, 23.2, 35.3, 125.1, 131.7: Silverstein, R. M.; Bassler, G. C.; Morrill, T. C. *Spectrometric Identification of Organic Compounds*; 1981; p 263.

[25] The observed peaks: 12.4, 13.7, 25.6, 28.9, 123.8, and 130.6 ppm; the literature values for *Z*-2-hexene: 12.6, 13.7, 22.6, 29.4, 124.0, 137.2: see citation in ref 24.

[26] Two sets of ^1H NMR peaks were observed: (a) 5.4−5.5 ppm (m) and 1.64 ppm (dd, $^3J_{H-H}$ = 4.8 Hz, $^4J_{H-H}$ = 1.2 Hz); (b) 5.4−5.5 ppm (m) and 1.61 ppm (q, $^3J_{H-H}$ = 5.0 Hz). Two sets of ^{13}C NMR peaks were also observed: (a) 125.8 and 17.8 ppm; (b) 124.6 and 12.4 ppm. These peaks are close to the literature values for *E*- (126.0 and 17.6 ppm) and *Z*- (124.6 and 12.1 ppm) 2-butenes (see citation in ref 24).

[27] $(PhSiH_2)_2$ was identified on the basis of the signal at 4.48 ppm, while $(PhMeSiH)_2$ showed signals at 4.45 ppm (br, 1 H) and 1.20 ppm (d, $^3J_{H-H}$ = 6.9 Hz, 3H): (a) Woo, H.-G.; Walzer, J. F.; Tilley, T. D. *J. Am. Chem. Soc.* **1992**, *114*, 7047. (b) Gauvin, F. Ph.D. Thesis, McGill University, 1992.

[28] Fontaine, F.-G.; Zargarian, D. *Organometallics* **2002**, *21*, 401.

PhMeSiH$_2$, polymerize Ph-CC-H, and isomerize 1-hexene. These results support our previous assertions that the dimerization of ethylene in systems consisting of IndNi(PPh$_3$)Cl/AgBF$_4$[4a] or IndNi(PPh$_3$)X/MAO[29] invovle cationic intermediates, while different intermediates are involved in the polymerization of phenylacetylene[12e] and ethylene[29] with the MAO-cocatalyzed systems. The facile substitution of the OTf moiety by a series of Lewis bases can also give the corresponding cationic adducts, some examples of which have been isolated and fully characterized. Studies are underway to probe and expand the scope of the reactions catalyzed by the OTf precursors.

Experimental Section

All manipulations and experiments were performed under an inert atmosphere using standard Schlenk techniques and/or in a nitrogen-filled glovebox. Dry, oxygen-free solvents were employed throughout. Bruker AMX400 and AV300 spectrometers were employed for recording ^{1}H (400 MHz), ^{13}C{^{1}H} (100.56 and 75.42 MHz), ^{19}F (376.31 MHz), and ^{31}P{^{1}H} (161.92 MHz) NMR spectra at ambient temperature. ^{1}H and ^{13}C{^{1}H} spectra are referenced to solvent resonances, ^{31}P{^{1}H} to 85% H_3PO_4, ^{19}F to $C_6H_5CF_3$ (−63.9 ppm). The IR spectra were taken on a Perkin-Elmer 1750 FTIR (4000−450 cm^{-1}) with sample prepared as KBr pellets or evaporated films on NaCl plates. Mass spectrometric measurements were performed by the Centre Régional de Spectrométrie de Masse de Université de Montréal. The elemental analyses were performed by Laboratoire d'Analyse Élémentaire (Université de Montréal). (1-Et-Ind)Ni(PPh$_3$)(thienyl), (1-*i*-Pr-Ind)Ni(PPh$_3$)(thienyl), (1-*i*-Pr-Ind)Ni(PPh$_3$)Cl, (1-Bz-Ind)Ni(PPh$_3$)(thienyl), and (1-Bz-Ind)-Ni(PPh$_3$)Cl were prepared as described elsewhere.[20] CF_3SO_3Ag, CF_3SO_3H, PPh$_3$, PMe$_3$, and CNC(CH$_3$)$_3$ were purchased from Aldrich and used as received. Pyridine, CH$_3$CN, and PhCN were purchased from A & C American Chemicals and were distilled from molecular sieves. CP grade carbon monoxide and ethylene (Praxair) were used without purification.

(1-Et-Ind)Ni(PPh$_3$)(OTf), 1. A CH$_2$Cl$_2$ solution (10 mL) of CF$_3$SO$_3$H (33.0 μL, 0.37 mmol) was added dropwise to the stirring CH$_2$Cl$_2$ solution (20 mL) of (1-Et-Ind)Ni(PPh$_3$)(thienyl) (201 mg, 0.37 mmol) at room temperature. The resulting red mixture was stirred for 10 min and filtered, and the filtrate evaporated to dryness. The residue was crystallized from CH$_2$Cl$_2$/hexane at room temperature to give the product as a red powder (120 mg, 52%). ^{1}H NMR (C$_6$D$_6$): 1.29 (t, $^3J_{H-H}$ = 7.3 Hz, −C*H*$_3$), 1.74 (m, −C*H*$_2$), 2.27 (m, −C*H*$_2$), 3.04 (s, H3), 5.80 (d, $^3J_{H-H}$ = 6.8 Hz, H4), 6.21 (d, $^3J_{H-H}$ = 2.6 Hz, H2), 6.75 (t, $^3J_{H-H}$ = 7.0 Hz, H5), 7.08 (t, $^3J_{H-H}$ = 7.4 Hz, H6), 7.00 (m, PPh$_3$), 7.38 (d, $^3J_{H-H}$ = 8.0 Hz, H7), 7.51 (m, PPh$_3$). ^{13}C NMR (CDCl$_3$, 300 MHz): 11.00 (CH$_2$*C*H$_3$), 20.19 (*C*H$_2$CH$_3$), 60.39 (C3), 102.27 (C2), 114.05 (d, $^2J_{P-C}$ = 11.3 Hz, C1), 117.66, 119.69, 127.38, 127.70, 128.18, 128.60 (d, $^3J_{P-C}$ = 9.9 Hz, *m*-PPh$_3$), 129.38, 129.89 (d, J_{P-C} = 44.4 Hz, *i*-PPh$_3$), 130.76 (s, *p*-PPh$_3$), 133.88 (d, $^2J_{P-C}$ = 11.8 Hz, *o*-PPh$_3$). ^{31}P{^{1}H} NMR (C$_6$D$_6$): 30.02 (s). ^{19}F{^{1}H} NMR (C$_6$D$_6$): −79.70 (s). FABMS (*m*/*z*): 463 (M$^+$ − OTf). Anal. Calcd for $C_{30}H_{26}PNiO_3SF_3$ (613.263): C, 58.76; H, 4.27, S, 5.23. Found: C, 58.60; H, 4.60, S, 4.66.

(1-*i*-Pr-Ind)Ni(PPh$_3$)(OTf), 2. Method A. A CH$_2$Cl$_2$ solution (10 mL) of CF$_3$SO$_3$H (23 μL, 0.249 mmol) was added dropwise to the stirring CH$_2$Cl$_2$ solution (20 mL) of (1-*i*-Pr-Ind)Ni(PPh$_3$)(thienyl) (140 mg, 0.249 mmol) at room temperature. The resulting red mixture was stirred for 30 min and filtered, and the filtrate evaporated to dryness. The residue was crystallized from CH$_2$Cl$_2$/hexane at room temperature to give the product as a red powder (68 mg, 44%).

Method B. The dark red solution of (1-*i*-Pr-Ind)Ni(PPh$_3$)-Cl (256 mg, 0.498 mmol) in CH$_2$Cl$_2$ (25 mL) was added to the stirring CH$_2$Cl$_2$ (15 mL) suspension of AgOTf (192 mg, 0.747 mmol). The resultant mixture was stirred for 2 h at room temperature and filtered, and the filtrate was evaporated to dryness. The residue was crystallized from C$_6$H$_6$/hexane at room temperature to give the product as a red powder (166 mg, 53%). Recrystallization of a small portion of this solid from a CH$_2$Cl$_2$/hexane solution at −20 °C yielded crystals suitable for X-ray diffraction studies. ^{1}H NMR (C$_6$D$_6$): 1.14 (d, $^3J_{H-H}$ = 7.0 Hz, −CH(C*H*$_3$)$_2$), 1.56 (d, $^3J_{H-H}$ = 6.5 Hz, −CH(C*H*$_3$)$_2$), 2.93 (m, −C*H*(CH$_3$)$_2$), 3.02 (tet, $^3J_{H-H}$ = 2.6 Hz, $^3J_{P-H}$ = 4.8 Hz, H3), 6.06 (d, $^3J_{H-H}$ = 7.8 Hz, H4), 6.14 (d, $^3J_{H-H}$ = 2.6 Hz, H2), 6.79 (t, $^3J_{H-H}$ = 7.9 Hz, H5), 7.01 (m, ArH), 7.18 (s, ArH), 7.51 (m, ArH). ^{13}C{^{1}H} NMR (CDCl$_3$, 300 MHz): 20.07 (CH(*C*H$_3$)$_2$), 20.90 (d, $^4J_{P-C}$ = 5.2 Hz, CH(*C*H$_3$)$_2$), 26.02 (s, *C*H(CH$_3$)$_2$), 61.44 (C3), 100.28 (C2), 117.98, 118.26, (d, $^2J_{P-C}$ = 11.3 Hz, C1), 120.63, 124.96 (C3a), 127.66 (C7a), 127.80, 128.51, 128.78 (d, $^3J_{P-C}$ = 10.3 Hz, *m*-PPh$_3$), 130.27 (d, $^1J_{P-C}$ = 44.2 Hz, *i*-PPh$_3$), 130.91 (s, *p*-PPh$_3$), 133.99 (d, $^2J_{P-C}$ = 11.9 Hz, *o*-PPh$_3$). ^{31}P{^{1}H} NMR: 29.30 (s) (in C$_6$D$_6$), 28.73 (s) (CDCl$_3$). ^{19}F{^{1}H} NMR: −79.79 (s) (in C$_6$D$_6$), −81.51 (s) (in CDCl$_3$). IR (KBr): 1637 (m), 1459 (m), 1481 (m), 1438 (s), 1385 (m), 1324 (m), 1252 (m), 1233 (s), 1213 (s), 1175 (s), 1121 (m), 1097 (m), 1031 (s), 749 (s), 725 (m), 695 (s), 639 (s), 543 (s), 532 (s), 511 (m), 495 (w). FABMS (*m*/*z*): 477 (M$^+$ − OTf). Anal. Calcd for $C_{31}H_{28}PNiO_3SF_3$ (627.289): C, 59.36; H, 4.50; S, 5.11. Found: C, 59.88; H, 4.53; S, 5.07.

(1-Bz-Ind)Ni(PPh$_3$)(OTf), 3. The dark red solution of (1-Bz-Ind)Ni(PPh$_3$)Cl (250 mg, 0.445 mmol) in CH$_2$Cl$_2$ (25 mL) was added to a stirred CH$_2$Cl$_2$ (15 mL) suspension of AgOTf (170 mg, 0.662 mmol). The resultant mixture was stirred for 2 h at room temperature and filtered, and the filtrate was evaporated to dryness. The residue was crystallized from C$_6$H$_6$/hexane at room temperature to give the product as a red powder (162 mg, 60%). ^{1}H NMR (C$_6$D$_6$): 3.00 (m, H3), 3.62 (dd, $^2J_{H--H}$ = 16.6 Hz, $^4J_{P-H}$ = 4.8 Hz, −C*H*$_2$-Ph), 3.34 (dd, $^2J_{H-H}$ = 16.6 Hz, $^4J_{P-H}$ = 4.8 Hz, −C*H*$_2$-Ph), 5.90 (d, $^3J_{H-H}$ = 7.4 Hz, H4), 6.09 (d, $^3J_{H-H}$ = 1.8 Hz, H2), 6.74 (t, $^3J_{H-H}$ = 7.9 Hz, H5), 7.00 (s, ArH), 7.08 (m, ArH), 7.42(d, *J* = 6.6 Hz, ArH), 7.49 (m, ArH). The complete characterization of this compound has been reported previously.[20]

[(1-*i*-Pr-Ind)Ni(PPh$_3$)(CH$_3$CN)]OTf, 4a. A CH$_2$Cl$_2$ solution (20 mL) of CH$_3$CN (15.5 μL, 0.296 mmol) was added dropwise to the stirring CH$_2$Cl$_2$ solution (10 mL) of (1-*i*-Pr-Ind)Ni(PPh$_3$)(OTf) (169 mg, 0.296 mmol) at room temperature. The resulting yellow mixture was stirred for 15 min, then evaporated to dryness. The orange oily residue was triturated in 15 mL of Et$_2$O at room temperature to give the product as a yellow powder (90 mg, 50%). The dark yellow crystals suitable for X-ray diffraction study were grown by vapor diffusion of pentane into a CHCl$_3$ solution of (1-*i*-Pr-Ind)Ni-(PPh$_3$)(CH$_3$CN)(OTf) at room temperature. ^{1}H NMR (CDCl$_3$): 1.38 (d, $^3J_{H-H}$ = 6.8 Hz, −CH(C*H*$_3$)$_2$), 1.44 (d, $^3J_{H-H}$ = 6.7 Hz, −CH(C*H*$_3$)$_2$), 1.99 (s, C*H*$_3$CN), 2.59 (m, C*H*(CH$_3$)$_2$), 4.18 (m, H3), 6.08 (d, $^3J_{H-H}$ = 7.8 Hz, H4), 6.36 (d, $^3J_{H-H}$ = 3.1 Hz, H2), 7.08 (t, $^3J_{H-H}$ = 7.3 Hz, H5), 7.26−7.55 (ArH). ^{13}C NMR (CDCl$_3$, 300 MHz): 14.05 (s, *C*H$_3$CN), 20.22 (CH(*C*H$_3$)$_2$), 21.40 (d, $^4J_{P-C}$ = 5.7 Hz, CH(*C*H$_3$)$_2$), 25.95 (s, *C*H(CH$_3$)$_2$), 71.66 (C3), 99.72 (C2), 117.56 (d, $^2J_{P-C}$ = 9.8 Hz, C1), 118.46, 119.34, 123.66 (C3a), 125.65 (C7a), 128.30, 128.69, 129.20 (d, $^3J_{P-C}$ = 10.4, *m*-PPh$_3$), 129.46, 130.84, 131.53 (d, $^4J_{P-C}$ = 1.9 Hz, *p*-PPh$_3$), 133.43 (d, $^2J_{P-C}$ = 11.9 Hz, *o*-PPh$_3$) 133.88. ^{31}P{^{1}H} NMR (CDCl$_3$): 34.94 (s). ^{19}F{^{1}H} NMR (CDCl$_3$): −80.62 (s). IR (KBr): 2251 (w, C═N), 1543 (w), 1480 (m), 1437 (s), 1385 (m), 1260 (s), 1160 (s), 1123 (m), 1098 (m), 1948 (m), 1034 (s), 1002 (w), 749 (s), 725 (m), 695 (s), 660 (m), 639 (s), 543 (s), 532 (s), 511 (m), 495 (w). FAB-MS *m*/*z* (%): 518.1 [(1-*i*-Pr-Ind)-Ni(PPh$_3$)(CH$_3$CN)]$^+$ (11), 477.1 [(1-*i*-Pr-Ind)Ni(PPh$_3$)]$^+$ (100).

---

(29) Dubois, M.-A.; Wang, R.; Zargarian, D.; Tian, J.; Vollmerhaus, R.; Li, Z.; Collins, S. *Organometallics* **2001**, *20*, 663.

Anal. Calcd for $\mathrm{C_{33}H_{31}PNiO_3SNF_3{\cdot}1.3CHCl_3}$ (823.533): C, 50.03; H, 3.95; S, 3.89; N, 1.70. Found: C, 49.99; H, 4.09; S, 3.93; N, 1.05.

[(1-*i*-Pr-Ind)Ni(PPh$_3$)(CD$_3$CN)]OTf, 4a′. $\mathrm{CD_3CN}$ (0.5 μL, 0.01 mmol) was added to the $\mathrm{CDCl_3}$ solution (0.5 mL) of (1-*i*-Pr-Ind)Ni($\mathrm{PPh_3}$)(OTf) (6 mg, 0.01 mmol) in an NMR tube. The color of the solution changed from red to yellow after the addition of $\mathrm{CD_3CN}$. ^{1}H NMR ($\mathrm{CDCl_3}$): 1.39 (d, $^3J_{\mathrm{H-H}} = 6.9$ Hz, $-\mathrm{CH}(\mathrm{C}H_3)_2$), 1.44 (d, $^3J_{\mathrm{H-H}} = 6.6$ Hz, $-\mathrm{CH}(\mathrm{C}H_3)_2$), 2.59 (m, $\mathrm{C}H(\mathrm{CH_3})_2$), 4.17 (m, H3), 6.08 (d, $^3J_{\mathrm{H-H}} = 8.0$ Hz, H4), 6.36 (d, $^3J_{\mathrm{H-H}} = 2.7$ Hz, H2), 7.08 (t, $^3J_{\mathrm{H-H}} = 7.3$ Hz, H5), 7.26−7.55 (m, ArH). ^{31}P{^{1}H} NMR ($\mathrm{CDCl_3}$): 34.97 (s). ^{19}F{^{1}H} NMR ($\mathrm{CDCl_3}$): −80.81 (s).

[(1-*i*-Pr-Ind)Ni(PPh$_3$)(CO)]OTf, 6a. Bubbling CO through a stirred $\mathrm{C_6H_6}$ solution (20 mL) of (1-*i*-Pr-Ind)Ni($\mathrm{PPh_3}$)(OTf) (150 mg, 0.239 mmol) at room temperature resulted in the precipitation of a yellow solid, which was filtered and washed twice with hexane to give a yellow powder (98 mg, 63%). ^{1}H NMR ($\mathrm{CDCl_3}$): 1.43 (d, $^3J_{\mathrm{H-H}} = 6.7$ Hz, $-\mathrm{CH}(\mathrm{C}H_3)_2$, 1.58 (d, $^3J_{\mathrm{H-H}} = 6.6$ Hz, $-\mathrm{CH}(\mathrm{C}H_3)_2$), 3.06 (m, $-\mathit{CH}(\mathrm{CH_3})_2$), 5.53 (m, H3), 6.11 (d, $^3J_{\mathrm{H-H}} = 8.0$ Hz, H4), 6.65 (d, $^3J_{\mathrm{H-H}} = 3.2$ Hz, H2), 7.26 (m, ArH), 7.53 (m, ArH). ^{13}C{^{1}H} NMR ($\mathrm{CDCl_3}$, 400 MHz): 21.50 ($\mathrm{CH}(\mathit{C}\mathrm{H_3})_2$), 22.93 (d, $^4J_{\mathrm{P-C}} = 6.4$ Hz, $\mathrm{CH}(\mathit{C}\mathrm{H_3})_2$), 27.22 (s, $\mathit{C}\mathrm{H(CH_3)_2}$), 91.77 (d, $^2J_{\mathrm{P-C}} = 3.2$ Hz, C3), 101.52 (d, $^2J_{\mathrm{P-C}} = 3.2$ Hz, C2), 117.84 (C3a), 119.09 (C7a), 119.83, 120.07, 120.25, 121.24, 121.40 (d, $^2J_{\mathrm{P-C}} = 10.6$ Hz, C1), 129.66 (d, $^3J_{\mathrm{P-C}} = 11.2$ Hz, *m*-PPh$_3$), 130.83 (d, $^1J_{\mathrm{P-C}} = 62.6$ Hz, *i*-PPh$_3$), 132.41 (d, $^4J_{\mathrm{P-C}} = 2.4$ Hz, *p*-PPh$_3$), 133.46 (d, $^2J_{\mathrm{P-C}} = 11.2$ Hz, *o*-PPh$_3$), 189.54 (d, $^2J_{\mathrm{P-C}} = 16.8$ Hz, *C*O). ^{31}P{^{1}H} NMR ($\mathrm{CDCl_3}$): 36.08 (s). ^{19}F{^{1}H} NMR ($\mathrm{CDCl_3}$): −79.57 (s). IR (KBr): 2089 (s), 1995 (m), 1638 (m), 1479 (m), 1460 (w), 1438 (s), 1385 (m), 1267 (s), 1173 (s), 1159 (s), 1121 (m), 1095 (m), 1045 (m), 747 (s), 754 (m), 725 (m), 696 (s), 637 (s), 544 (m), 531 (m), 516 (m). FAB-MS *m*/*z* (%): 505.1 [(1-*i*-Pr-Ind)Ni(PPh$_3$)(CO)]$^+$ (100), 477.1 [(1-*i*-Pr-Ind)Ni(PPh$_3$)]$^+$ (98). Anal. Calcd for $\mathrm{C_{32}H_{28}PNiO_4SF_3}$ (655.30): C, 58.65; H, 4.31; S, 4.89. Found: C, 58.16; H, 3.84; S, 4.90.

(1-*i*-Pr-Ind)Ni(PPh$_3$)(Py)(OTf), 7a. A $\mathrm{C_6H_6}$ solution (20 mL) of pyridine (19.3 μL, 0.239 mmol) was added dropwise to the stirred $\mathrm{C_6H_6}$ solution (10 mL) of (1-*i*-Pr-Ind)Ni($\mathrm{PPh_3}$)(OTf) (150 mg, 0.239 mmol) at room temperature. The resulting orange mixture was stirred for 5 min, then evaporated to dryness. The orange oily residue was triturated in 15 mL of $\mathrm{Et_2O}$ at room temperature to give the product as a yellow powder (110 mg, 65%). ^{1}H NMR ($\mathrm{CDCl_3}$): 1.12 (d, $^3J_{\mathrm{H-H}} = 6.5$ Hz, $-\mathrm{CH}(\mathrm{C}H_3)_2$), 1.17 (d, $^3J_{\mathrm{H-H}} = 6.8$ Hz, $-\mathrm{CH}(\mathrm{C}H_3)_2$), 1.44 (m, $-\mathit{CH}(\mathrm{CH_3})_2$), 4.21 (m, H3), 6.18 (d, $^3J_{\mathrm{H-H}} = 7.6$ Hz, H4), 6.75 (d, $^3J_{\mathrm{H-H}} = 2.6$ Hz, H2), 7.09−7.87 (m, ArH), 8.60 (s, PyH). ^{31}P{^{1}H} NMR ($\mathrm{CDCl_3}$): 32.84 (s). ^{19}F{^{1}H} NMR ($\mathrm{CDCl_3}$): −79.45 (s). ^{13}C{^{1}H} NMR ($\mathrm{CDCl_3}$, 300 MHz): 19.76 ($\mathrm{CH}(\mathit{C}\mathrm{H_3})_2$), 21.23 ($\mathrm{CH}(\mathit{C}\mathrm{H_3})_2$), 25.74 ($\mathit{C}\mathrm{H(CH_3)_2}$), 68.32 (C3), 101.39 (C2), 115.28 (d, $^2J_{\mathrm{P-C}} = 10.6$ Hz, C1), 117.72 (C3a), 119.57 (C7a), 125.16, 126.00, 128.07, 128.75 (d, $^1J_{\mathrm{P-C}} = 45.39$ Hz, *i*-PPh$_3$), 129.16 (d, $^3J_{\mathrm{P-C}} = 10.2$ Hz, *m*-PPh$_3$), 130.80, 131.24 (d, $^4J_{\mathrm{P-C}} = 2.3$ Hz, *p*-PPh$_3$), 133.21 (d, $^2J_{\mathrm{P-C}} = 11.2$ Hz, *o*-PPh$_3$), 133.84, 138.57 (b, Py), 152.19 (Py). FAB-MS *m*/*z* (%): 556.2 [(1-*i*-Pr-Ind)Ni(PPh$_3$)(Py)]$^+$ (76), 477.1 [(1-*i*-Pr-Ind)Ni(PPh$_3$)]$^+$ (100), 399.1 [Ni(PPh$_3$)(Py)]$^+$ (16). Anal. Calcd for $\mathrm{C_{36}H_{33}PNiO_3SNF_3}$ (706.391): C, 61.21; H, 4.71; S, 4.54; N, 1.98. Found: C, 60.84; H, 4.96; S, 4.00; N, 1.96.

(1-*i*-Pr-Ind)Ni(PPh$_3$)(CNC(CH$_3$)$_3$)(OTf), 8a. A $\mathrm{C_6H_6}$ solution (20 mL) of $\mathrm{CNC(CH_3)_3}$ (29.4 μL, 0.260 mmol) was added dropwise to the stirred $\mathrm{C_6H_6}$ solution (10 mL) of (1-*i*-Pr-Ind)-Ni($\mathrm{PPh_3}$)(OTf) (200 mg, 0.319 mmol) at room temperature. After 5 min, the resulting orange mixture was concentrated to precipitate the desired product, which was filtered and washed twice with pentane to afford a yellow powder (100 mg, 54%). Crystals suitable for X-ray diffraction studies were grown by the slow (room temperature) evaporation of a toluene/$\mathrm{CDCl_3}$ mixture. ^{1}H NMR ($\mathrm{CDCl_3}$): 1.01 (s, $\mathrm{CNC}(\mathrm{C}H_3)_3$), 1.40 (d, $^3J_{\mathrm{H-H}} = 6.9$ Hz, $-\mathrm{CH}(\mathrm{C}H_3)_2$), 1.50 (d, $^3J_{\mathrm{H-H}} = 6.6$ Hz, $-\mathrm{CH}(\mathrm{C}H_3)_2$), 2.84 (m, $-\mathit{CH}(\mathrm{CH_3})_2$), 4.80 (m, H3), 6.14 (d, $^3J_{\mathrm{H-H}} = 7.6$ Hz, H4), 6.27 (d, $^3J_{\mathrm{H-H}} = 3.0$ Hz, H2), 7.19−7.56 (m, ArH). ^{13}C{^{1}H} NMR ($\mathrm{CDCl_3}$, 300 MHz): 21.53 ($\mathrm{CH}(\mathit{C}\mathrm{H_3})_2$), 22.04 (d, $^4J_{\mathrm{P-C}} = 4.2$ Hz, $\mathrm{CH}(\mathit{C}\mathrm{H_3})_2$), 27.18 (s, $\mathit{C}\mathrm{H(CH_3)_2}$), 29.81 ($\mathrm{CNC}(\mathit{C}\mathrm{H_3})_3$), 59.75 ($\mathrm{CN}\mathit{C}\mathrm{(CH_3)_3}$), 82.90 (C3), 99.51 (C2), 115.29 (d, $^2J_{\mathrm{P-C}} = 10.6$ Hz, C1), 119.22, 120.48 (C3a), 121.99 (C7a), 129.12, 129.28, 129.65 (d, $^3J_{\mathrm{P-C}} = 10.8$ Hz, *m*-PPh$_3$), 129.81, 130.45, 132.31 (d, $^4J_{\mathrm{P-C}} = 2.4$ Hz, *p*-PPh$_3$), 133.81 (d, $^2J_{\mathrm{P-C}} = 11.3$ Hz, *o*-PPh$_3$). ^{31}P{^{1}H} NMR ($\mathrm{CDCl_3}$): 38.11 (s). ^{19}F{^{1}H} NMR ($\mathrm{CDCl_3}$): −79.47 (s). IR (KBr): 2196 (s, $C{=}N$), 1630 (w), 1479 (m), 1437 (m), 1385 (s), 1272 (s), 1223 (m), 1185 (w), 1148 (s), 1121 (w), 1098 (m), 1032 (s), 999 (w), 765 (m), 754 (m), 697 (s), 638 (s), 533 (s), 510 (s). Anal. Calcd for $\mathrm{C_{36}H_{37}PNiO_3SNF_3}$ (710.422): C, 60.86; H, 5.25; S, 4.51; N, 1.97. Found: C, 60.95; H, 5.38; S, 4.22; N, 2.07.

[(1-*i*-Pr-Ind)Ni(PPh$_3$)$_2$](OTf), 9a. Dropwise addition of a $\mathrm{C_6H_6}$ solution (20 mL) of $\mathrm{PPh_3}$ (64 mg, 0.246 mmol) to the stirred $\mathrm{C_6H_6}$ solution (10 mL) of (1-*i*-Pr-Ind)Ni($\mathrm{PPh_3}$)(OTf) (150 mg, 0.239 mmol) at room temperature resulted in the precipitation of a dark yellow solid. Recrystallization of this solid from $\mathrm{CH_2Cl_2}$/hexane gave the desired product (162 mg, 76%). ^{1}H NMR ($\mathrm{CDCl_3}$): 0.85 (d, $^3J_{\mathrm{H-H}} = 6.3$ Hz, $-\mathrm{CH}(\mathrm{C}H_3)_2$), 1.14 (d, $^3J_{\mathrm{H-H}} = 6.2$ Hz, $-\mathrm{CH}(\mathrm{C}H_3)_2$), 0.78 (m, $-\mathit{CH}(\mathrm{CH_3})_2$), 5.13 (m, H3), 5.54 (d, $J_{\mathrm{H-H}} = 7.7$ Hz, ArH), 6.60 (d, $J_{\mathrm{H-H}} = 7.9$ Hz, ArH), 6.74 (d, $J_{\mathrm{H-H}} = 3.2$ Hz, ArH), 7.00 (m, ArH) 7.13−7.60 (m, ArH). ^{31}P{^{1}H} NMR ($\mathrm{CDCl_3}$): 34.97 (d, $^2J_{\mathrm{p-p}} = 25.4$ Hz), 29.78 (d, $^2J_{\mathrm{p-p}} = 25.4$ Hz). ^{19}F{^{1}H} NMR ($\mathrm{CDCl_3}$): −79.37 (s). FAB-MS *m*/*z* (%): 739.2 [(1-*i*-Pr-Ind)Ni(PPh$_3$)$_2$]$^+$ (76), 477.2 [(1-*i*-Pr-Ind)Ni(PPh$_3$)]$^+$ (100), 582.1 [Ni(PPh$_3$)$_2$]$^+$ (34).

The Remaining Adducts. In a number of cases, the substitution of OTf in **2** or **3** by L was monitored spectroscopically, without isolating the resulting adducts. These reactions were carried out by adding 1 equiv of L (except for CO, which was bubbled through for 2−3 min) to a 0.5 mL $\mathrm{CDCl_3}$ solution of **2** or **3** (ca. 0.015 mmol) in an NMR tube. The NMR spectra of these samples were then measured at room temperature. The data are given below.

[(1-Bz-Ind)Ni(PPh$_3$)(CH$_3$CN)]OTf, 4b. ^{1}H NMR ($\mathrm{CDCl_3}$): 1.96 (b, $\mathrm{C}H_3\mathrm{CN}$), 3.47 (dd, $^2J_{\mathrm{H-H}} = 14.3$ Hz, $^4J_{\mathrm{P-H}} = 2.5$ Hz, $-\mathrm{C}H_2$-Ph), 3.58 (dd, $^2J_{\mathrm{H-H}} = 14.3$ Hz, $^4J_{\mathrm{P-H}} = 2.5$ Hz, $-\mathrm{C}H_2$-Ph), 4.16 (m, H3), 6.04 (d, $^3J_{\mathrm{H-H}} = 7.7$ Hz, H4), 6.42 (d, $^3J_{\mathrm{H-H}} = 2.5$ Hz, H2), 7.06 (t, $^3J_{\mathrm{H-H}} = 7.4$ Hz), 7.34−7.49 (m, ArH). ^{31}P{^{1}H} NMR ($\mathrm{CDCl_3}$): 34.93 (s). ^{19}F{^{1}H} NMR ($\mathrm{CDCl_3}$): −79.33 (s).

[(1-*i*-Pr-Ind)Ni(PPh$_3$)(PhCN)]OTf, 5a. ^{1}H NMR ($\mathrm{CDCl_3}$): 1.29 (d, $^3J_{\mathrm{H-H}} = 6.7$ Hz, $-\mathrm{CH}(\mathrm{C}H_3)_2$), 1.38 (d, $^3J_{\mathrm{H-H}} = 6.6$ Hz, $-\mathrm{CH}(\mathrm{C}H_3)_2$), 2.45 (m, $-\mathit{CH}(\mathrm{CH_3})_2$),), 4.21 (m, H3), 5.95 (d, $^3J_{\mathrm{H-H}} = 6.6$ Hz, H4), 6.37 (d, $^3J_{\mathrm{H-H}} = 2.9$ Hz, H2), 6.87−7.38 (m, ArH). ^{31}P{^{1}H} NMR ($\mathrm{CDCl_3}$): 35.21 (s). ^{19}F{^{1}H} NMR ($\mathrm{CDCl_3}$): −79.61 (s).

[(1-Bz-Ind)Ni(PPh$_3$)(PhCN)]OTf, 5b. ^{1}H NMR ($\mathrm{CDCl_3}$): 3.45 (d, $^2J_{\mathrm{H-H}} = 15.4$ Hz, $-\mathrm{C}H_2$-Ph), 3.75 (d, $^2J_{\mathrm{H-H}} = 15.4$ Hz, $-\mathrm{C}H_2$-Ph), 4.30 (m, H3), 6.05 (d, $^3J_{\mathrm{H-H}} = 7.8$ Hz, H4), 6.65 (d, $^3J_{\mathrm{H-H}} = 1.8$ Hz, H2), 7.11 (t, $^3J_{\mathrm{H-H}} = 7.4$ Hz), 7.26−7.64 (m, ArH). ^{31}P{^{1}H} NMR ($\mathrm{CDCl_3}$): 35.25 (s). ^{19}F{^{1}H} NMR ($\mathrm{CDCl_3}$): −79.41 (s).

[(1-Bz-Ind)Ni(PPh$_3$)(CO)]OTf, 6b. ^{1}H NMR ($\mathrm{CDCl_3}$): 3.92 (d, $^2J_{\mathrm{H-H}} = 14.2$ Hz, $-\mathrm{C}H_2$-Ph), 4.35 (d, $^2J_{\mathrm{H-H}} = 14.2$ Hz, $-\mathrm{C}H_2$-Ph), 5.35 (m, H3), 5.99 (d, $^3J_{\mathrm{H-H}} = 7.4$ Hz, H4), 6.90−7.68 (m, ArH). ^{31}P{^{1}H} NMR ($\mathrm{CDCl_3}$): 36.23 (s). ^{19}F{^{1}H} NMR ($\mathrm{CDCl_3}$): −79.48 (s).

[(1-Bz-Ind)Ni(PPh$_3$)(Py)]OTf), 7b. ^{1}H NMR ($\mathrm{CDCl_3}$): 2.31 (dd, $^2J_{\mathrm{H-H}} = 15.0$ Hz, $^4J_{\mathrm{P-H}} = 3.0$ Hz, $-\mathrm{C}H_2$-Ph), 3.29 (dd, $^2J_{\mathrm{H-H}} = 15.0$ Hz, $^4J_{\mathrm{P-H}} = 2.2$ Hz, $-\mathrm{C}H_2$-Ph), 4.21 (m, H3), 6.25 (d, $^3J_{\mathrm{H-H}} = 7.8$ Hz, H4), 7.12−8.62 (m, ArH). ^{31}P{^{1}H} NMR ($\mathrm{CDCl_3}$): 31.98(s). ^{19}F{^{1}H} NMR ($\mathrm{CDCl_3}$): −79.45 (s).

[(1-Bz-Ind)Ni(PPh$_3$)(CNC(CH$_3$)$_3$)]OTf, 8b. ^{31}P{^{1}H} NMR ($\mathrm{CDCl_3}$): 38.11 (s). ^{19}F{^{1}H} NMR ($\mathrm{CDCl_3}$): −79.47(s).

[(1-Bz-Ind)Ni(PPh$_3$)$_2$]OTf, 9b. ^{1}H NMR ($\mathrm{CDCl_3}$): 2.27 (d, $^2J_{\mathrm{H-H}} = 14.3$ Hz, $-\mathrm{C}H_2$-Ph), 3.03 (d, $^2J_{\mathrm{H-H}} = 14.3$ Hz, $-\mathrm{C}H_2$-Ph), 5.04 (m, H3), 6.00 (d, $J_{\mathrm{H-H}} = 7.2$ Hz, ArH), 6.28 (d, $J_{\mathrm{H-H}}$

= 7.1 Hz, ArH), 6.92 (d, $J_{H-H} = 7.2$ Hz, ArH), 7.08−7.43 (m, ArH). $^{31}P\{^1H\}$ NMR ($CDCl_3$): 35.17 (d, $^2J_{p-p} = 25.5$ Hz), 32.12 (d, $^2J_{p-p} = 25.5$ Hz). $^{19}F\{^1H\}$ NMR ($CDCl_3$): −79.27 (s).

[(1-*i*-Pr-Ind)Ni(PPh₃)(PMe₃)]OTf, 10a. $^{31}P\{^1H\}$ NMR ($CDCl_3$): 41.69 (d, $^2J_{p-p} = 42.0$ Hz), −10.44 (d, $^2J_{p-p} = 42.0$ Hz); −8,71 (d, $^2J_{p-p} = 42.0$ Hz), 15.01 (d, $^2J_{p-p} = 42.0$ Hz).

[(1-Bz-Ind)Ni(PPh₃)(PMe₃)]OTf, 10b. $^{31}P\{^1H\}$ NMR ($CDCl_3$): 41.27 (d, $^2J_{p-p} = 42.0$ Hz), −10.26 (d, $^2J_{p-p} = 42.0$ Hz); 40.86 (d, $^2J_{p-p} = 43.3$ Hz), −17.03 (d, $^2J_{p-p} = 43.3$ Hz). $^{19}F\{^1H\}$ NMR ($CDCl_3$): −79.52 (s).

Reaction of 2 with 1-Hexene. NMR spectroscopy was used to monitor the reaction of 1-hexene (0.1 mL, 0.80 mmol, 1.6 M in $CDCl_3$) and **2** (10 mg, 0.016 mmol, 0.032 M in $CDCl_3$). The $^{13}C\{^1H\}$ NMR spectra indicated a slow isomerization of 1-hexene (ca. 24 h) to mostly *E*-2-hexene (13.6, 17.9, 22.7, 34.8, 124.7, and 131.4 ppm) and another minor isomer (12.4, 13.7, 25.6, 28.9, 123.8, and 130.6 ppm). The GC/MS analysis of the NMR mixture or that of a CH_2Cl_2 solution of 1-hexene (0.2 mL, 1.6 mmol) and **2** (20 mg, 0.032 mmol) showed the presence of hexenes and traces of 1,3-(hexenyl, *i*-propyl)-indene ($M^{\bullet+}$ = 240; $M^{\bullet+}$ − 15 (CH_3); $M^{\bullet+}$ − 29 (CH_2CH_3); $M^{\bullet+}$ − 43 (Pr or *i*-Pr); $M^{\bullet+}$ − 57 (Bu); etc.).

Dimerization of Ethylene Catalyzed by 2. A $CDCl_3$ solution of **2** (30 mg, 0.048 mmol, in 2 mL) was saturated with ethylene (ca. 5 min) prior to analysis by NMR and GC/MS. ^1H NMR ($CDCl_3$): 1.61 (d, $^3J_{H-H} = 5.0$, CH_3 of *Z*-butene), 1.64 (dd, $^3J_{H-H} = 5.0$, $^4J_{H-H} = 1.2$, CH_3 of *E*-butene), 5.44 (m, vinylic H for both *Z*- and *E*-butenes). The GC/Ms showed both butenes (predominant) and another species that displayed the fragmentation pattern consistent with (isopropyl, vinyl)indene: $M^{\bullet+}$ (184, $C_{14}H_{16}$), $M^{\bullet+}$ − 15 ($C_{13}H_{13}$), $M^{\bullet+}$ − 43 ($C_{11}H_9$), $M^{\bullet+}$ − 56 ($C_{10}H_8$), $M^{\bullet+}$ − 69 (C_9H_7).

Polymerization of PhCCH. A mixture of Ph-CC-H (1.08 mL, 9.6 mmol) and **2** (30 mg, 0.048 mmol) was stirred for 24 h at 50 °C. Addition of MeOH to the mixture gave an oily yellow solid, which was filtered and recrystallized from THF/MeOH to give a yellow powder (ca. 5% yield). Similar results were obtained when the reaction was carried out with the same Ni:substrate ratio but in THF. Analysis of the product obtained from the neat reaction by GPC gave the following data: $M_w = 8189$, $M_n = 4418$, $M_w/M_n = 1.85$. The ^1H NMR spectrum of this solid showed a broad, featureless signal at ca. 6.5−7.8 ppm.

Dimerization of Silanes Catalyzed by 2. PhSiH₃. To a C_6D_6 solution of **2** (10 mg, 0.016 mmol, 0.032 M) was added $PhSiH_3$ (0.20 mL, 1.6 mmol) and the sample shaken to ensure mixing. A red to brown color change was observed. Analysis by ^1H NMR showed that only a small amount of $PhSiH_3$ (<5 equiv) had been converted to the dimer (δ 4.48, b, $PhSiH_2$). Analysis by $^{31}P\{^1H\}$ NMR showed the presence of a peak at 40.18 ppm.

Ph(Me)SiH₂. To a C_6D_6 solution of **2** (10 mg, 0.016 mmol, 0.032 M) was added $Ph(Me)SiH_2$ (0.020 mL, 0.14 mmol) and the sample shaken to ensure mixing. A red to brown color change was observed. Analysis by ^1H NMR showed that only a small amount of $Ph(Me)SiH_2$ (<5 equiv) had been converted to the dimer (δ 1.20 (d, $^3J_{H-H} = 6.9$ Hz, Me), 4.45 (b, Si*H*)).

X-ray Diffraction Studies of 2, 4a, and 8a. Dark red crystals of **2** were grown from a CH_2Cl_2/hexane solution at −20 °C; the crystals of **2** did not decompose after exposure to air for 21 days. Dark yellow crystals of **4a** were grown by vapor diffusion of pentane into a $CHCl_3$ solution at room temperature; complex **4a** cocrystallized with one molecule of $CHCl_3$ in each unit cell. Dark yellow crystals of **8a** suitable for X-ray diffraction study were grown by vapor diffusion of pentane into a $CHCl_3$ solution at room temperature. The crystallographic data (Table 1) were collected on a Bruker AXS SMART 2K diffractometer with graphite-monochromated Cu Kα radiation at 293(2) K using SMART.[30] Cell refinement and data reduction were done using SAINT.[31] The structures were solved by direct methods using SHELXS97[32] and difmap synthesis using SHELXL96;[33] refinements were done on F^2 by full-matrix least squares. The OTf group and $CHCl_3$ molecule in **4a** are disordered. Similarly, the OTf anion and the three methyl groups on the isocyanide ligand in **8a** are disordered, too. Complete crystallographic data for these three structures are included in the Supporting Information.

Acknowledgment. We are grateful to the NSERC of Canada, the FCAR of Québec, and Université de Montréal for financial support, to Prof. Hélène Lebel and Valérie Paquet for GC/MS analyses, and to Jake Dalphond and Dr. H. Sleiman for GPC.

Supporting Information Available: Complete details on the X-ray analyses of **2**, **4a**, and **8a**, including tables of bond distances and angles, anisotropic thermal parameters, and hydrogen atom coordinates. These materials are available free of charge via the Internet at http://pubs.acs.org.

OM020558A

---

[30] *SMART*, Release 5.059; Bruker Molecular Analysis Research Tool; Bruker AXS Inc.: Madison, WI, 53719-1173, 1999.

[31] *SAINT*, Release 6.06; Integration Software for Single-Crystal Data; Bruker AXS Inc.: Madison, WI, 53719-1173, 1999.

[32] Sheldrick, G. M. *SHELXS*, Program for the Solution of Crystal Structures; University of Goettingen: Germany, 1997.

[33] Sheldrick, G. M. *SHELXL*, Program for the Refinement of Crystal Structures; University of Goettingen: Germany, 1996.